

Implications of neutrino species number and summed mass measurements in cosmological observations

N. Sasao* and M. Yoshimura†

Research Institute for Interdisciplinary Science, Okayama University, Tushima-naka 3-1, Kita-ku Okayama 700-8530,

M. Tanaka‡

*Department of Physics, Graduate School of Science,
Osaka University, Toyonaka, Osaka 560-0043, Japan*

(Dated: August 27, 2024)

We confront measurable neutrino degrees of freedom N_{eff} and summed neutrino mass in the early universe to particle physics at the energy scale beyond the standard model (BSM), in particular including the issue of neutrino mass type distinction. The Majorana-type of massive neutrino is perfectly acceptable by Planck observations, while the Dirac-type neutrino may survive in a restricted class of models that suppresses extra right-handed contribution to $\Delta N_{\text{eff}} = N_{\text{eff}} - 3$ at a nearly indistinguishable level from the Majorana case. There is a chance that supersymmetry energy scale may be identified in supersymmetric extension of left-right symmetric model if improved N_{eff} measurements discover a finite value. Combined analysis of this quantity with the summed neutrino mass helps to determine the neutrino mass ordering pattern, if measurement accuracy of order, $60 \sim 80$ meV, is achieved, as in CMB-S4.

I. INTRODUCTION

Discovery of non-vanishing neutrino masses by oscillation experiments requires extension of the electroweak standard model based on massless left-handed ν_L neutrinos. In general, both left and right handed neutrino fields, ν_L^i ($i = 1, 2, 3$ for the three neutrino scheme) and ν_R^i are introduced in this extension. Difference of Dirac and Majorana types of neutrino is in whether projected two-component mass eigenstates have mass degeneracy (Dirac case), or have two distinct masses $m(\nu_R^i) \neq m(\nu_L^i)$ (Majorana case), large and small ones. The mass degeneracy of Dirac neutrinos implies the law of lepton number conservation, while the Majorana neutrino violates the lepton number conservation.

The Majorana case provides the interesting seesaw mechanism explaining why ordinary neutrinos appearing in weak processes are very light (typically much smaller than $m_\nu/m_e = O(10^{-7})$ with m_e the electron mass) compared to all other fermions, being suppressed in proportion to $1/m(\nu_R)$ by heavy ν_R masses, $m(\nu_R)$'s [1]. The lepton number violation has a further consequence of interesting leptogenesis scenario which explains the baryon asymmetry of our universe [2]. In this scenario the final baryon and the lepton number asymmetries are comparable in their magnitudes, of order 10^{-10} , and excludes a possibility of large chemical potential for leptons. Experimental determination of Majorana or Dirac neutrino is thus one of the most outstanding problems that faces particle physics.

The plausible three-neutrino scheme predicts the neutrino species number $N_{\text{eff}} = 3$ (for a small deviation, see

the note [3]) at nucleosynthesis for three species of Majorana neutrinos. On the other hand, if the independent ν_R component in the Dirac-type neutrino fully contributes to the extra of neutrino species, the Dirac theory would predict $N_{\text{eff}} = 6$ in contradiction to cosmological observations. What usually happens is that ν_R decouples earlier from the rest of thermal particles, and after a series of subsequent reheating events their number density decreases relative to ν_L still in thermal equilibrium. The extent of diluted ν_R number density is estimated by the adiabatic relation of entropy conservation, and it gives an extra contribution to $\Delta N_{\text{eff}} = N_{\text{eff}} - 3$, usually time and temperature dependent, after ν_L decoupling.

Planck observations of cosmic microwave background (CMB) provided a stringent value $N_{\text{eff}} = 2.99 \pm 0.17$ at 1σ CL [4]. This result is perfectly consistent with the Majorana-type neutrino, but barely consistent with the Dirac-type neutrino. There have been some discussions of how to understand this and a less stringent 2σ result, $2.99^{+0.34}_{-0.33}$, if the neutrino mass is of Dirac type since Planck publication [5], [6], [7], [8]. We shall recapitulate the Dirac-type neutrino case improving calculation of ν_R decoupling temperature. Precision N_{eff} measurements in cosmological observations of CMB-S4 [9] is expected to determine this number accurately.

Improved future measurements including null result are expected to probe species number present in physics beyond the standard model (BSM), if the neutrino mass of Dirac type. We find it of particular interest to target supersymmetric extension of left-right symmetric model. In this case it becomes possible to identify SUSY scale if a finite ΔN_{eff} is found, or lower energy scale if it is not found.

Our further task in the present paper is a combined analysis of the neutrino species number and the summed neutrino mass measurement: irrespective of Majorana or Dirac neutrinos, the analysis is shown to have a great im-

* sasao@okayama-u.ac.jp

† yoshim@okayama-u.ac.jp

‡ tanaka@phys.sci.osaka-u.ac.jp

pact on the neutrino mass ordering problem, the normal hierarchy (NH) or the inverted hierarchy (IH). We shall be able to provide a new perspective of what forthcoming observations imply to BSM physics.

The present paper is organized as follows. In the next section we explain some basic facts about the neutrino species number N_{eff} , and what cosmological observations of this quantity imply. The adiabatic entropy conservation is emphasized and calculation of the relativistic degrees of freedom $g_*(T)$ in thermal medium of temperature T becomes important. The Majorana-type of massive neutrino is found compatible with cosmological observations, while the Dirac-type neutrino requires new analysis, as done in the literature. In Section III theoretical framework for discussion of Dirac-type massive neutrino is pointed out. Calculation of right-handed ν_R decoupling in this framework is worked out in detail, since results in the literature lack details of these calculations. We present detailed explanation of ν_R production, adding processes not considered in the literature. It is shown that four-Fermi type approximation of ν_R pair production rate is sufficient to determine the thermalization condition and the decoupling temperature. In Section IV we discuss how the derived decoupling temperature is related to diluted ΔN_{eff} and the necessary dilution may be realized in unification schemes. We may relate SUSY energy scale to ΔN_{eff} and shall be able to discuss how supersymmetric left-right symmetric schemes are constrained. In Section V another important quantity of summed neutrino masses in future cosmological observations may be combined to neutrino oscillation data, and resulting plot in $(\Delta N_{\text{eff}}, \sum_i m_i)$ plane can be used to determine another neutrino property, normal and inverted mass hierarchical ordering.

Throughout this paper we use the unit of $\hbar = c = k_B = 1$.

II. PRELIMINARY

A. N_{eff} at nucleosynthesis and at epochs after recombination

The effective massless degrees of freedom N_{eff} determines the cosmic energy density, hence controls the speed of cosmic expansion. This quantity at nucleosynthesis (~ 100 seconds since the big-bang) is measurable by comparing measured light element abundances with theoretical calculation, while the same quantity at later epochs after recombination ($\sim 4 \times 10^5$ years after the bang) is measured by Planck and CMB-S4 observations. The quantity N_{eff} at these two epochs is sensitive function of ${}^4\text{He}$ abundance Y_p . The allowed region in the (Y_p, N_{eff}) plane from observations is usually presented by contour maps. The important fact is that correlations given by the derivative signs of dN_{eff}/dY_p are opposite at two epochs, positive at nucleosynthesis and negative at recombination. This makes it possible to determine both

of N_{eff} and Y_p at high precision.

The primordial ${}^4\text{He}$ abundance Y_p is around 0.25. Reference [10] on nucleosynthesis cites a conservative bound $N_{\text{eff}} < 4$, but also mentions a more restrictive bound $N_{\text{eff}} < 3.2$. The correlation with Y_p at nucleosynthesis gives a straight line in the (N_{eff}, Y_p) plane, as reviewed in [9], ranging in $N_{\text{eff}} = 2.2 \sim 3.4$. The final status of Planck 2018 + BAO observations gives an impressive upper bound $N_{\text{eff}} < 3.33$ at 95% CL [4].

Not only neutrinos, but also other stable light relics left behind from the early thermal history give additional contribution, extra $\Delta N_{\text{eff}} = 0.03 \sim 0.05$ per a single relic. Examples are axion, dark photon and sterile neutrino. Contribution from a spin-less stable light relic is $\Delta N_{\text{eff}} \sim 0.027$. This quantity can also be negative if light relics are unstable and decay during two epochs. We shall assume that there is no such relic, or even if there is, their cumulative contribution is restricted at most by $|\Delta N_{\text{eff}}| < 0.028$ (CMB-S4 target value), and concentrate on diluted Dirac ν_R which may behave in a similar way to a light relic.

B. Adiabatic dilution factor and ΔN_{eff}

Assume that ν_R in the Dirac theory is thermally abundant at early cosmological epochs, and calculate the amount of dilution. After ν_R decoupling the universe goes through many annihilation events of thermal antiparticles, thereby reheating the universe. Electroweak interaction is far stronger than interactions in BSM, hence left-handed ν_L is reheated, but ν_R is not. This gives rise to difference of ν_L and ν_R effective temperatures. Note that even after ν_R 's decouple and become non-thermal, one can assign their effective temperature. This is because the entropy conservation of $a^3 s(T)$ (with $a(t)$ the time-dependent cosmic scale factor) holds at nearly instantaneous reheating processes. The entropy density $s(T)$ is proportional to the massless degrees of freedom $g_*(T)$ in radiation-dominated epoch. Hence one can readily calculate the temperature ratio before and after reheating events by counting respective species number contributing to g_* .

Assuming that the standard electroweak phase transition took place in the Big Bang Universe, it is straightforward to evaluate g_* in the era up to the electroweak phase transition in the standard model.

Fermions are counted by the weight 7/8 for one spin state and bosons by the weight 1. Counting $g_*(T)$ gives the dilution factor in terms of number density ratio, $n(\nu_R)/n(\nu_L) = 43/427 = 0.101$, since the electroweak phase transition.

We summarize g_* factors relevant to ν_R dilution in the following table, Table(I) in which g_*^i indicates the species number at cosmological events i . It is convenient in the rest of analysis to relate the extra ΔN_{eff} to the extra

i	ν_L	EW	ν_R	S4
g_*^i	10.75	106.75	124.75	360
ΔN_{eff}^i	3	0.14	0.11	0.028

TABLE I. Species number g_*^i with i indicating cosmological events at which ν_R decoupling occur simultaneously (in an approximate sense). i = ν_L being left-handed neutrino decoupling, EW standard model phase transition, ν_R the phase transition of the doublet left-right symmetric model, while g_*^{S4} is the expected species number that can be probed by CMB-S4. The formula $3(g_*^{\nu_L}/g_*^i)^{4/3}$ is used for ΔN_{eff}^i .

relativistic degrees of freedom Δg_* ,

$$\left(\frac{g_*^{\text{EW}} + \Delta g_*}{g_*^{\nu_L}}\right)^{-4/3} = \frac{\Delta N_{\text{eff}}}{3}, \quad (1)$$

where $g_*^{\text{EW}} = 427/4$ is the species number of electroweak theory, and $g_*^{\nu_L} = 43/4$. Note that Δg_* can be negative, implying that ν_R decoupling may occur below the electroweak temperature $T^{\text{EW}} \sim 250$ GeV.

Alternatively, one can relate ΔN_{eff} upper bound or observed value to required Δg_* value, using the formula (1).

III. FATE OF RIGHT-HANDED NEUTRINO OF DIRAC TYPE

A. Theory of Dirac-type massive neutrino

Let us first recall what happens in the standard electroweak theory based on the gauge group $\text{SU}(2)_L \times \text{U}(1)$, when one introduces the right-handed neutrino ν_R . It is known that introduction of $\text{SU}(2)_L \times \text{U}(1)$ singlet ν_R opens the possibility of Higgs boson (h) coupling proportional to doublet bi-linear fermion ($\bar{\nu}_L, \bar{l}_L$) ν_R which, after the spontaneous electroweak gauge symmetry breaking, gives the Dirac-type neutrino mass. Inevitable process $\nu_L h \rightarrow \nu_R$ from thermal ν_L, h produces ν_R , but with a negligible amount of ν_R ($\Delta N_{\text{eff}} \ll 0.05$) if neutrino masses are less than of order 100 eV [10]. There seems nothing wrong with this scheme, but this minimum extension does not give any clue to many outstanding problems of particle physics such as generation of the baryon asymmetry. We need a new theoretical framework of massive Dirac-type neutrino.

A natural scheme is grand unified gauge theories (GUT), but it is sufficient to first think of an intermediate step of subgroup unification towards GUT. We find it most natural to analyze ν_R dilution in the left-right symmetric extension of the standard electroweak theory, $\text{SU}(2)_R \times \text{SU}(2)_L \times \text{U}(1)$ gauge theory [11], as also made in [7]. The Higgs system consists of irreducible representations, $(2, 2), (2, 1), (1, 2)$ of $\text{SU}(2)_R \times \text{SU}(2)_L$ group. Regarding all species of particle as massless, there are 18 extra g_* in addition to the standard one 427/4 and three right-handed neutrinos 21/4.

Some details of this doublet left-right symmetric model (DLRSM) are given in Appendix.

B. Decoupling of thermalized right-handed neutrinos in LR symmetric model

The Boltzmann equation for the number density, obtained after integrating the distribution function $f(\vec{p})$ in the phase space (space volume times the momentum-space volume $d^3p/(2\pi)^3$ in spatially homogeneous universe), describes time evolution in the expanding universe. Consider a number density of f species n_f . The equations is

$$\dot{n}_f + 3H(T)n_f = \sum_i \Gamma_i n_{i \neq f} - \Gamma_f n_f, \quad (2)$$

with $H(T)$ the Hubble rate $\sqrt{\frac{8\pi G_N}{3}}\rho_r$ (ρ_r the energy density of effectively massless particles, $\pi^2 g_* T^4/30$). When the Hubble rate $H(T)$ compared with right-hand side (RHS) is small, thermal equilibrium is realized with vanishing RHS of (2) (meaning the positive production and the negative destruction balance). This thermal equilibrium is ended at decoupling temperature T_d^f that is determined by equating the rate to the Hubble rate, $H(T_d^f) = \Gamma_R$. One may use for ν_R annihilation rate Γ_R

$$\Gamma_R(T) = \frac{16}{n_R(T)} \int \frac{d^3p_1 d^3p_2}{4p_1 p_2 (2\pi)^6} \frac{\mathcal{S}}{(e^{p_1/T} + 1)(e^{p_2/T} + 1)} \quad (3)$$

$$\mathcal{S} = \int \frac{d^3q_1 d^3q_2}{4q_1 q_2 (2\pi)^2} \delta^{(4)}(p_1 + p_2 - q_1 - q_2) \mathcal{R}(s, t). \quad (4)$$

Momenta of initial and final particles, assumed massless, are denoted $p_i, q_i, i = 1, 2$, respectively. Lorentz-invariant squared amplitude $\mathcal{R}(s, t)$ summed over spin states is written in terms of invariant variables, $s = (p_1 + p_2)^2, t = (p_1 - q_1)^2$. They are calculated below. $n_R(T) = 3\zeta(3)(2s_p + 1)T^3/4\pi^2$ is the number density of initial thermal ν_R ($s_p = 1/2$ is its spin).

One may separately confirm that thermalization condition is satisfied by considering inverse processes. Since we treat all initial and final fermions as massless (actually much lighter than gauge bosons W_R, Z_R) inverse ν_R production process has equal rate to the annihilation rate. Thus, time integrated quantity $n_R \Gamma_R$ gives thermally summed ν_R number density.

Relevant annihilation processes of right-handed neutrino ν_R (conjugate processes of $\bar{\nu}_R$ production to be included as well) in LR symmetric models occur via two-body colliding processes of many kinds. Typical Feynman diagrams are depicted in Fig(1). In order to calcu-

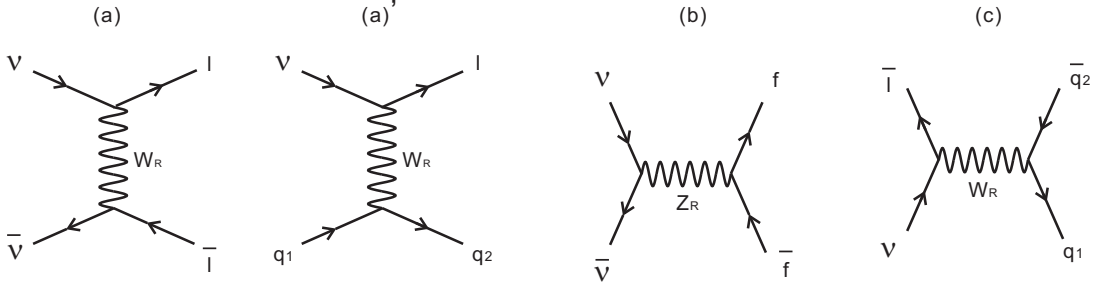


FIG. 1. Typical Feynman diagrams: (a) $\nu_R \bar{\nu}_R \rightarrow l_R \bar{l}_R$ (t-channel W_R exchange), (a') $\nu_R q_R^1 \rightarrow l_R q_R^2$, $(q_1, q_2) = (d, u), (s, c), (b, t)$ (t-channel W_R exchange), (b) $\nu_R \bar{\nu}_R \rightarrow f_R \bar{f}_R$, $f = q, l$ (s-channel Z_R exchange), (c) additional s-channel W_R exchange contribution, $\nu_R \bar{l}_R \rightarrow q_R^1 \bar{q}_R^2$, $(q_1, q_2) = (u, d), (c, s), (t, b)$, $l = e, \mu, \tau$.

late rate, we classify individual contributions as

$$(a); (al); \nu_R \bar{\nu}'_R \rightarrow l_R \bar{l}'_R, (aq) : \nu_R \bar{u}_R \rightarrow l_R \bar{d}_R, \quad (t\text{-channel } W\text{-exchange}), \quad (5)$$

$$(a)'; \nu_R d_R \rightarrow l_R u_R, (t\text{-channel } W\text{-exchange}), \quad (6)$$

$$(b); \nu_R \bar{\nu}_R \rightarrow f_R \bar{f}_R, (s\text{-channel } Z\text{-exchange}), \quad (7)$$

$$(b)'; \nu_R \bar{\nu}_R \rightarrow f_L \bar{f}_L, (s\text{-channel } Z\text{-exchange}), \quad (8)$$

$$(c); \nu_R \bar{l}_R \rightarrow u_R \bar{d}_R, (s\text{-channel } W\text{-exchange}), \quad (9)$$

with $f = q, l$ being quarks and charged lepton. We note that process involving light higgs pair is absent, because a neutral scalar field has no vector current that may couple to Z_R . Feynman rules for amplitude and rate calculation can readily be extracted using formulas in Appendix.

A part of these contributions to annihilation rates have been calculated in the literature. Their substantial part is missing in the literature, and we shall cover and add all relevant contributions. The decoupling temperature T_d at which two rates are equal is related to right-handed gauge coupling masses and gauge coupling g_R . Remarkably, we shall be able to provide analytic results for important quantities we need.

$SU(2)_R \times SU(2)_L \times U(1)$ gauge theory gives contributions from (a) \sim (c) listed in (5) \sim (9), some of them depicted in Fig(1). Invariant squared amplitudes $\mathcal{R}(s, t)$ after spin summation consist of coupling factors and dynamical parts given in terms of s, t variables. Listed contributions have different s, t dependence. It is sufficient to calculate $\mathcal{R}(s, t)$ in the temperature range $T \ll$ gauge boson masses, hence four-Fermi approximation is excellent, with the common strength factor G_R ,

$$\frac{g_R^4}{M_Z^4 \cos^2 \theta_R} = \frac{g_R^4}{M_W^4} \equiv 32 G_R^2. \quad (10)$$

We used notations M_W, M_Z for W_R, Z_R masses, to distinguish from ordinary electroweak gauge bosons m_W, m_Z , and g_R, θ_R are gauge coupling constant and mixing angle in the $SU(2)_R$ sector. Flavor dependent

coupling factors are further multiplied to squared Fermi constant;

$$C_{2t}^{al} = \frac{3}{4}, \quad C_{2t}^{aq} = \frac{9}{4}, \quad C_{2t}^{a'} = \frac{9}{4}, \quad (11)$$

$$C_{2s}^b = \frac{1}{4} \left(9 \left(\frac{1}{2} - \frac{2}{3} \sin^2 \theta_R \right)^2 + 9 \left(-\frac{1}{2} + \frac{1}{3} \sin^2 \theta_R \right)^2 + 3 \left(-\frac{1}{2} + \sin^2 \theta_R \right)^2 \right), \quad (12)$$

$$C_{2s}^{b'} = \frac{1}{4} \left(18 \left(-\frac{\sin^2 \theta_R}{6} \right)^2 + 6 \left(\frac{\sin^2 \theta_R}{2} \right)^2 \right), \quad (13)$$

$$C_{2s}^c = \frac{9}{4}, \quad C_{st} = \frac{1}{4} \left(-\frac{1}{2} + \sin^2 \theta_R \right). \quad (14)$$

Contributions C_φ^α in squared amplitudes arise from α -type of diagrams in Fig(1) and those of φ -type of exchanged gauge bosons. For instance, C_{2t}^{aq} is from squared t-channel exchange of Fig(1a) in which leptons l are replaced by relevant quarks q .

The last coupling C_{st} arises from interference contribution of t-channel W_R -exchange (a) diagram and s-channel Z_R -exchange (b) diagram for two-body process of $\nu_R \bar{\nu}_R \rightarrow l_R \bar{l}_R$, $l = e, \mu, \tau$. As explained in Appendix, a value $\sin^2 \theta_R = 0.299$ should be used. Using these couplings, squared invariant amplitudes are given by

$$\mathcal{R}(s, t) = 32 G_R^2 \left(C_{2t}^{a'} s^2 + (C_{2t}^{al} + C_{2t}^{aq})(s+t)^2 + C_{2s}^b (s+t)^2 + C_{2s}^{b'} t^2 + C_{2s}^c (s+t)^2 - 2 C_{st} (s+t)^2 \right) \quad (15)$$

The last integral over final states in (4) is to be calculated in general coordinate frames. If one replaces this by the total cross section in the center-of-mass frame, the important part of asymmetric collisions between initial fermion pairs is lost.

The angular integration over final state variables is done in Lorentz-invariant manner, which gives trivial angular integrations, $\int (s+t)^2 = \int t^2 = \frac{1}{3} s^2$, $\int s^2 = s^2$.

Thus, the annihilation cross section is

$$\begin{aligned}\sigma v &= 4 \frac{1}{2p_1 p_2} \frac{1}{16\pi s} \int_{-s}^0 dt \mathcal{R}(s, t) \\ &= \frac{4G_R^2}{\pi} \frac{s^2}{p_1 p_2} \left(C_{2t}^{a'} + \frac{1}{3} (C_{2t}^{al} + C_{2t}^{aq} \right. \\ &\quad \left. + C_{2s}^b + C_{2s}^{b'} + C_{2s}^c - 2C_{st}) \right). \quad (16)\end{aligned}$$

Using $s = 2p_1 p_2 (1 - \cos \theta_{12})$, the angular integral in the initial state gives $4\pi^2 \int_0^{4p_1 p_2} ds/p_1 p_2$. Finally, integration over initial thermal fermions leads to

$$\begin{aligned}\Gamma_R &= \frac{49\pi^5}{3\zeta(3) \cdot 675} G_R^2 T^5 I(\sin^2 \theta_R) \\ &= 26.2 G_R^2 T^5, \quad I(x) = \frac{1}{48} (217 - 56x + 40x^2) \quad (17)\end{aligned}$$

using the value of $x = \sin^2 \theta_R = 0.299$, given in Appendix.

We presented results using exact Fermi-Dirac (FD) distribution function for fundamental fermions, quarks and leptons. In Appendix, we also derive results taking the approximate Maxwell-Boltzmann (MB) distribution, which gives analytic results that differ by

$$\left(\frac{\int_0^\infty dx x^3 e^{-x}}{\int_0^\infty dx x^3 / (e^x + 1)} \right)^2 = \frac{518400}{49\pi^8} = 1.11499, \quad (18)$$

The result of annihilation rate divided by n_f is 0.9948 times FD value, two values being surprisingly close to each other within 1% difference.

Some comments on thermal distribution function may be in order. After copious production right-handed neutrinos scatter with thermal particles (via Z_R exchange) and their energies are redistributed. Thus, ν_R thermal distribution function is realized with zero chemical potential. Thermal gauge bosons W_R can produce ν_R , but they decouple much earlier, resulting in no further thermal ν_R production.

We have also calculated ν_R production rates in a much more simplified approximation of using thermally averaged values in the invariant total cross section σv . Using the averaged $\bar{t} = -s/2$, $\bar{t}^2 = s^2/3$, one has the thermally averaged $\sigma v = \bar{S}/4p_1 p_2$ given by

$$\sigma v = \frac{4G_R^2}{\pi} s I(\sin^2 \theta_R). \quad (19)$$

This gives $\Gamma_R \approx 6\zeta(3)G_R^2 \bar{s} I/\pi^3$. The thermal average of s is $\bar{s} = 2\bar{p}^2 = 1.814T^2$, hence one derives $\Gamma_R \sim 1.79G_R^2 T^5$, which grossly differs from the more precise result (17). This estimate confirms the importance of asymmetric collision in rate calculations. Note that one is not allowed to take the center of mass frame in the comoving frame of thermal universe, since head-on collisions do not necessarily occur and collisions with angles do occur usually. Thus, one has to perform thermal

average over angular configurations. The invariant variables $s = 2E_1 E_2 (1 - \cos \theta_{12})$, $t = -2E_1 E_2 (1 - \cos \theta_{13})$ of a massless (1, 2) pair collision (1, 2) \rightarrow (3, 4) must be averaged using thermal distribution functions of fermions, $1/(e^{E_i/T} + 1)$.

ν_R production rate Γ_R may be compared to the Hubble rate,

$$H(T) = \sqrt{\frac{4\pi^3}{45} g_*(T)} \frac{T^2}{m_{\text{pl}}}. \quad (20)$$

The decoupling temperature $T_d^{\nu_R}$ is defined by equating two rates: $\Gamma_R(T_d^{\nu_R}) = H(T_d^{\nu_R})$ gives

$$T_d^{\nu_R} = 3.8 \text{ MeV} \left(\frac{G_R^{-1/2}}{\text{TeV}} \right)^{4/3} \left(\frac{g_*^{\nu_R}}{g_*^{\text{EW}}} \right)^{1/6}. \quad (21)$$

Using the cited value $\sim 550 \text{ MeV}$ of Planck-BAO limit [5], one may derive a limit on $G_R^{-1/2} > 42 \text{ TeV} (g_*^{\nu_R}/g_*^{\text{EW}})^{-1/8}$.

The decoupling temperature of right-handed neutrinos is discussed in the literature [5–8]. Among them, Ref. [7] treats of the DLRS as in the present work. It is difficult to compare our decoupling temperature with that in Ref. [7], since it has not given details of how to calculate ν_R annihilation rate. We, however, obtain a considerably smaller decoupling temperature than that of Ref. [7] by a few orders of magnitude.

ν_R contributes to an extra ΔN_{eff} given by

$$\frac{\Delta N_{\text{eff}}}{3} = \left(\frac{g_*^{\nu_R}}{g_*^{\text{EW}}} \right)^{-4/3}, \quad (22)$$

with $g_*^{\nu_L} = 10.75$ (species number at left-handed neutrino decoupling). If ν_R decoupling occurs below the electroweak scale 250 GeV, one has $\Delta N_{\text{eff}} > 0.14$ since $g_*(T^{\text{EW}})/g_*^{\nu_L} = 9.93$, a value slightly smaller than Planck limit, but much larger than CMB-S4 target value 0.028. One can eliminate $g_*^{\nu_R}$ in favor of measurable ΔN_{eff} , to give

$$T_d^{\nu_R} = 2.95 \text{ MeV} \left(\frac{G_R^{-1/2}}{\text{TeV}} \right)^{4/3} \Delta N_{\text{eff}}^{-1/8}. \quad (23)$$

Calculations so far are based on that thermal environment consists of fundamental quarks and leptons. This picture is valid at temperatures above $\sim 200 \text{ MeV}$ at which hadronization occurs and quarks are incorporated into hadrons, namely baryons and mesons. This restricts the applicable region of unification scale to

$$G_R^{-1/2} > 20 \text{ TeV} \left(\frac{g_*^{\text{EW}}}{g_*^{\nu_R}} \right)^{1/8}. \quad (24)$$

For $G_R^{-1/2}$ outside this region the predicted ΔN_{eff} is grossly inconsistent with Planck observations. The LR symmetric unification, if the Majorana option is disfavored, thus appears at energy scale above $O(10^4) \text{ GeV}$, far beyond the electroweak scale.

IV. FURTHER UNIFICATION FOR SUFFICIENT DILUTION

We assume that ν_R decoupling occurs above the electroweak scale, hence $\Delta g_* = g_*^{\nu_R} - g_*^{\text{EW}} > 0$. A rational for this assumption is that species dilution below the electroweak scale is much limited, and forthcoming ΔN_{eff} observations would readily reject the scenario of ν_R decoupling below electroweak scale, as seen in Table(I).

There exists an obvious inequality $\Delta g_* \leq g_*^{\text{tot}} - g_*^{\text{EW}}$, with g_*^{tot} the total effective relativistic degrees of freedom in an extended gauge theory, resulting in $\Delta g_* \leq 18$ and corresponding $\Delta N_{\text{eff}} = 0.114$ in the minimum LR symmetric model. Thus, if a value of $\Delta N_{\text{eff}} < 0.1$ is measured, this would exclude the minimum LR symmetric model of Dirac-type neutrino.

A high energy scale decoupling by imposing $T_d^{\nu_R} > 250$ GeV (electroweak scale) in (23) leads to

$$G_R^{-1/2} > 5.0 \times 10^3 \text{ TeV} (\Delta N_{\text{eff}})^{3/32}, \quad (25)$$

giving the right-hand side limit, 3.7×10^3 TeV for $\Delta N_{\text{eff}} = 0.05$ (twice of CMB-S4 target value), corresponding to $g_*^{\nu_R} = 230$ from (22), a nearly doubled species value of standard electroweak theory.

Note that the Planck 1σ limit of ΔN_{eff} is 0.16. The minimum $\text{SU}(2)_R \times \text{SU}(2)_L \times \text{U}(1)$ model gives too small Δg_* . It is interesting that measured ΔN_{eff} , hence theoretically inferred Δg_* from a improved measured value, can determine how large one should think of in terms of degrees of freedom in Dirac-type neutrino models.

Since no sizable dilution factor is expected in the DLRSM model, one needs a proliferated particle spectrum beyond the electroweak scale. There are a few possibilities: minimum supersymmetric extension of standard model (MSSM) [12, 13], grand unified theories (GUT) and supersymmetric GUT [14]. For simplicity we assume that there is only one new energy scale beyond the electroweak scale. The important question is where the new energy scale lies and how much the dilution factor is.

We focus on the MSSM and assume for simplicity a single energy scale M_S where all super-partners of standard model particles emerge. Total $g_* = 228.75$ in MSSM, $2.143 \times$ standard model value. In order to estimate ν_R decoupling temperature, it is necessary to incorporate new contributions to ν_R annihilation rate caused by super-partners. R-parity conservation in SUSY restricts the number of contributing diagrams: there are two additional diagrams to each of classified DLRSM models given in (5) \sim (9) that contain two super-partners either in final or initial states. Examples of MSSM diagrams are shown in Fig(2).

Kinematic variable dependence of cross sections may differ for massless bosons and massless fermions, for instance in differential cross sections. Summation over initial thermal particles is also different for bosons and

fermions due to their equilibrium distribution functions. Incorporating this change of rate in MSSM gives ν_R decoupling temperature modified by $O(3^{-1/3})$, and the new energy scale

$$G_R^{-1/2} > 4.9 \times 10^3 \text{ TeV} \left(\frac{\Delta N_{\text{eff}}}{0.05}\right)^{3/32} \left(\frac{X}{3}\right)^{1/4}, \quad (26)$$

with X of order 3, but expected to deviate slightly. Thus, the number of diagrams in MSSM are essentially tripled.

Suppose that CMB-S4 did not find new contributions and set an upper limit $\Delta N_{\text{eff}} < 0.028$ at 1σ level. As shown in Fig(3), MSSM extension of DLRSM cannot save models of Dirac-type neutrinos. Nonetheless, Majorana-type neutrino models are acceptable. Similar arguments in $\text{SO}(10)$ models [16] based on proliferated species of $g_* = 710$ show that GUT scale of order 10^{16} GeV is acceptable to accommodate DLRSM structure. Thus, CMB-S4 is expected to have a great impact on physics beyond standard model.

V. COMBINED ANALYSIS USING SUMMED NEUTRINO MASS MEASUREMENT

Extra ΔN_{eff} due to relic ν_R contributes to the summed neutrino masses, which is also a target of forthcoming CMB-S4 observations.

It is of great value to summarize analyzed data using the minimum neutrino mass value defined as m_0 . Neutrino oscillation data gives the summed neutrino mass in terms of different functions of m_0 , with different offset parameters in the normal hierarchical (NH) and the inverted hierarchical (IH) orderings;

$$\frac{\sum_i m_i}{1 + \frac{\Delta N_{\text{eff}}}{3}} = m_0 + \sqrt{8.61^2 + m_0^2} + \sqrt{50.1^2 + m_0^2}, \quad (27)$$

for NH, and

$$\frac{\sum_i m_i}{1 + \frac{\Delta N_{\text{eff}}}{3}} = m_0 + \sqrt{50.0^2 + m_0^2} + \sqrt{49.2^2 + m_0^2}, \quad (28)$$

for IH, where mass values are given in meV unit. We note that $\sum_i m_i$ denotes the summed neutrino mass determined by cosmological observations. This quantity should be divided by the dilution factor to compare with the values of the oscillation experiments[15]. Offset values given by setting $m_0 = 0$ are > 58.7 and > 99.2 meV, for NH and IH, respectively. This difference in two ordering schemes is significantly large.

In Fig(4) we show the region in the $(\Delta N_{\text{eff}}, \sum_i m_i)$ plane allowed by Planck 2018 observations. These results hold irrespective of whether neutrinos are of Majorana or of Dirac type, since neutrino oscillation data cannot distinguish these two types. Nevertheless, plots given here can help NH and IH differences in future cosmological observations.

In the case of Dirac-type neutrino one can add more to this. One can readily convert ΔN_{eff} to Δg_* using

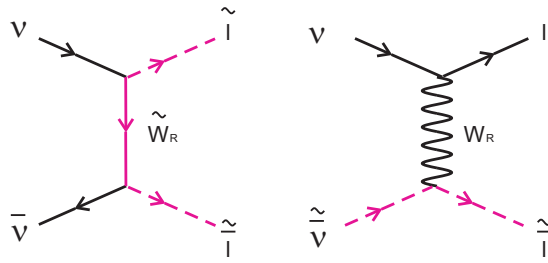


FIG. 2. Examples of SUSY Feynman diagrams. Super partners are shown in magenda.

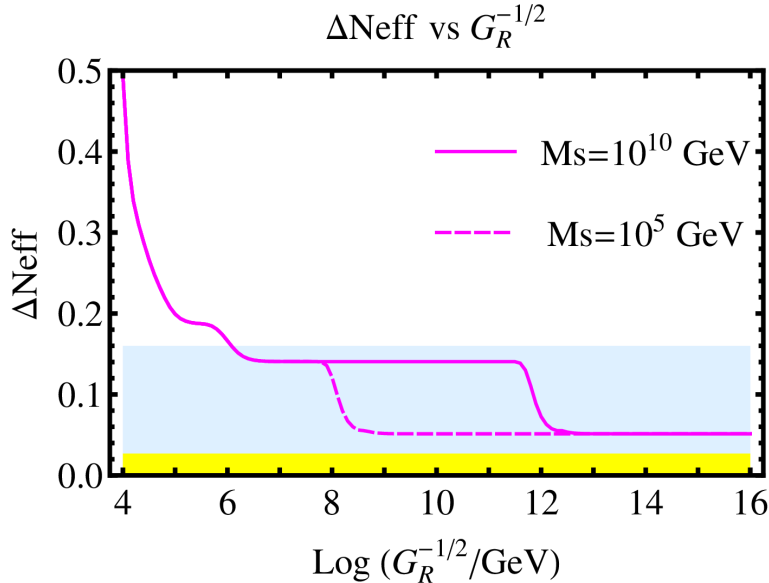


FIG. 3. Plot of ΔN_{eff} vs the logarithm of $G_R^{-1/2}/\text{GeV}$. MSSM particles of a single mass $M_s = 10^{10}$ GeV in solid magenda and 10^5 GeV in dotted magenta are taken, and species nearly doubled from the standard model are assumed together with $X = 3$ in (26). The blue band is for Planck 2018 at 1σ upper bound, while the yellow band is for $\Delta N_{\text{eff}} = 0.028$ CMB-S4 expectation.

(1) in favor of theoretical convenience of Dirac-type neutrino. We illustrate results in Fig(4) for three choices of the smallest neutrino mass. With improved accuracy in future observations one can reject IH schemes of larger smallest mass more readily than NH schemes. The minimum LR symmetric model is on the verge of rejection if IH scheme is adopted.

Considering these forecasts of cosmological observations, direct experiments of the smallest mass measurement and M/D distinction in terrestrial laboratories becomes even more important. It has been proposed to use laser-initiated coherence to measure these in atomic experiments in order to enhance otherwise tiny rates [18].

In summary, we investigated how cosmological observations of neutrino properties can probe still undetermined neutrino mass types and measure mass parame-

ters with precision, under a few plausible assumptions: (1) three neutrino scheme, (2) zero chemical potential of thermal particles, (3) no hypothetical light relic or relics with small accumulated contribution to ΔN_{eff} less than ~ 0.05 .

The Majorana neutrino, with rapid decay of its heavy right-handed partners, is in agreement with cosmological observations at nucleo-synthesis and at later epochs after recombination. But, Dirac-type right-handed neutrinos ν_R 's, must be diluted away, to give $\Delta N_{\text{eff}} < 0.16$, as limited by Planck + DESI observations. The necessary dilution is provided by reheating left-handed neutrino after cosmological ν_R decoupling, hence the problem is sensitive to particle content in thermal equilibrium. It is necessary, for the answer to this question, to identify a proper theoretical framework of how right-handed neutrino bound is satisfied. We find it most natural to adopt gauge theories including $SU(2)_R \times SU(2)_L \times U(1)$ as a subgroup, and how a nearly complete dilution of ν_R may oc-

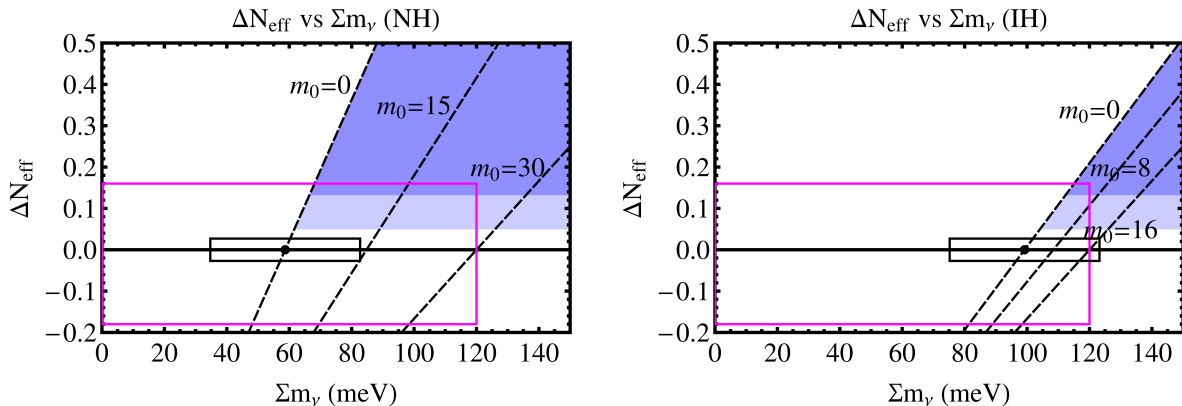


FIG. 4. Plot of ΔN_{eff} vs $\sum m_\nu$ for NH (left panel) and IH (right panel). The large rectangular box in magenta indicates the current 1σ limits on ΔN_{eff} and $\sum m_\nu$, determined by Planck 2018 [4]. The small rectangular box in black shows the anticipated $\pm 1\sigma$ errors by future observations [9]. The center point would move inside or around the large rectangular box depending on the outcome of the observations. The three dashed lines are the ΔN_{eff} -vs- $\sum m_\nu$ relations, given in Eqs. (27) and (28), with m_0 indicated in the figure. The dark and light blue shaded areas indicate the allowed regions of the DLRSM and its MSSM extension with sufficiently high decoupling temperature, respectively.

cur, requiring a prolific set of particles as large as $O(100)$.

Implication of CMB-S4 sensitivity $\Delta N_{\text{eff}} \sim 0.028$ in Dirac-type neutrino models is that either $SU(2)_R \times SU(2)_L \times U(1)$ is extended by supersymmetry allowing ~ 2 dilution after decoupling or grand unified extension of the left-right symmetric models is required as typical favored cases, thus making it possible to explore highest energy scale of particle physics.

The choice of NH or IH mass ordering scheme, irrespective of the mass types, should not be too difficult to determine in CMB-S4 observations.

Note added.

After completion of this work we became aware of the work, DESI Collaboration, arXiv:2404/03002v2[astro-ph[CO], in which analysis of DESI observations suggests that 72 meV is likely to be the upper bound of summed neutrino mass. This makes the right panel IH case in our Fig(4) disfavored.

ACKNOWLEDGMENTS

We appreciate O. Tajima at Kyoto University for valuable information and comments on CMB-S4 and other projects. This research was partially supported by Grant-in-Aid 19H00686 (NS), 18K03621 (MT), and 21K03575 (MY) from the Japanese Ministry of Education, Culture, Sports, Science, and Technology.

Appendix A: Doublet left-right symmetric model

1. Gauge symmetry and matter contents

The gauge symmetry of doublet left-right symmetric model (DLRSM) is

$$SU(3)_C \times SU(2)_L \times SU(2)_R \times U(1)_{B-L}. \quad (\text{A1})$$

The fermions in DLRSM are

$$Q_L = \begin{pmatrix} u_L \\ d_L \end{pmatrix}, \quad Q_R = \begin{pmatrix} u_R \\ d_R \end{pmatrix}, \quad (\text{A2})$$

$$L_L = \begin{pmatrix} \nu_L \\ \ell_L \end{pmatrix}, \quad L_R = \begin{pmatrix} \nu_R \\ \ell_R \end{pmatrix}, \quad (\text{A3})$$

where gauge quantum numbers of underlying group are $(3, 2, 1, 1/3)$, $(3, 1, 2, 1/3)$, $(1, 2, 1, -1)$, $(1, 1, 2, -1)$, respectively for quarks Q_L, Q_R and leptons L_L, L_R .

Three types of scalars in DLRSM are introduced:

$$\Phi = \begin{pmatrix} \phi_1^0 & \phi_2^+ \\ \phi_1^- & \phi_2^0 \end{pmatrix} : (1, 2, 2, 0), \quad (\text{A4})$$

$$\chi_L = \begin{pmatrix} \chi_L^+ \\ \chi_L^0 \end{pmatrix} : (1, 2, 1, 1), \quad (\text{A5})$$

$$\chi_R = \begin{pmatrix} \chi_R^+ \\ \chi_R^0 \end{pmatrix} : (1, 1, 2, 1). \quad (\text{A6})$$

2. Spontaneous symmetry breaking (SSB)

The vacuum expectation values

$$\langle \Phi \rangle = \begin{pmatrix} v_1/\sqrt{2} & 0 \\ 0 & v_2/\sqrt{2} \end{pmatrix}, \quad (\text{A7})$$

$$\langle \chi_L \rangle = \begin{pmatrix} 0 \\ v_L/\sqrt{2} \end{pmatrix}, \quad (\text{A8})$$

$$\langle \chi_R \rangle = \begin{pmatrix} 0 \\ v_R/\sqrt{2} \end{pmatrix}, \quad (\text{A9})$$

with a fine-tuning inequality $v_R \gg v_1, v_2, v_L$ lead to the following SSB pattern:

$$\begin{aligned} & \text{SU}(2)_L \times \text{SU}(2)_R \times \text{U}(1)_{\text{B-L}} \xrightarrow{v_R} \text{SU}(2)_L \times \text{U}(1)_Y \\ & \xrightarrow{v_{1,2,L}} \text{U}(1)_{\text{em}}. \end{aligned} \quad (\text{A10})$$

The first step is relevant to the study of ν_R decoupling above the electroweak scale $v^2 = v_1^2 + v_2^2 + v_L^2 \simeq (246 \text{ GeV})^2$.

With a fine-tuning $v \ll v_R$ there is only one light Higgs boson h of mass in the electroweak energy scale, while all other Higgs bosons remain much heavier than electroweak scale.

3. Nonstandard gauge bosons

In addition to the gauge bosons in the standard model, we have a pair of charged gauge bosons $W_{R\mu}^\pm$ and a neutral gauge boson $Z_{R\mu}$ in the DLRSB. The mass eigenstates are expressed in terms of the gauge basis field as

$$W_{R\mu}^\pm = \frac{1}{2}(W_{R\mu}^1 \mp W_{R\mu}^2), \quad (\text{A11})$$

$$Z_{R\mu} = \frac{1}{g_{Z_R}}(g_R W_{R\mu}^3 - g_{\text{B-L}} B_{\text{B-L}\mu}), \quad (\text{A12})$$

$$g_{Z_R} = \sqrt{g_R^2 + g_{\text{B-L}}^2}, \quad (\text{A13})$$

where g_R and $g_{\text{B-L}}$ are the gauge coupling constants of $\text{SU}(2)_R$ and $\text{U}(1)_{\text{B-L}}$ respectively. Their masses are given by

$$M_W = \frac{1}{2}g_R v_R, \quad M_Z = \frac{1}{2}g_{Z_R} v_R. \quad (\text{A14})$$

Incidentally, the $\text{U}(1)_Y$ gauge boson is identified as the orthogonal state of Z_R as

$$B_\mu = \frac{1}{g_{Z_R}}(g_{\text{B-L}} W_{R\mu}^3 + g_R B_{\text{B-L}\mu}), \quad (\text{A15})$$

and it is massless at this stage. With the gauge mixing angle defined by

$$\tan \theta_R = \frac{g_{\text{B-L}}}{g_R}, \quad (\text{A16})$$

one may express the neutral gauge bosons in the gauge basis in terms of those in the mass basis as

$$W_{R\mu}^3 = Z_{R\mu} \cos \theta_R + B_\mu \sin \theta_R, \quad (\text{A17})$$

$$B_{\text{B-L}\mu} = -Z_{R\mu} \sin \theta_R + B_\mu \cos \theta_R. \quad (\text{A18})$$

4. Nonstandard gauge interactions of fermions

The kinetic term of fermions is

$$\mathcal{L}_f = \bar{f} i \not{D} f, \quad (\text{A19})$$

with the covariant derivative D_μ given by

$$\begin{aligned} D_\mu &= \partial_\mu + i g_L T_L^a W_{L\mu}^a + i g_R T_R^a W_{R\mu}^a \\ &+ i \frac{g_{\text{B-L}}}{2} (B - L) B_{\text{B-L}\mu}, \\ &= \partial_\mu + i g_L T_L^a W_{L\mu}^a + i g_Y Y B_\mu \\ &+ i \frac{g_R}{\sqrt{2}} (T_R^+ W_{R\mu}^+ + T_R^- W_{R\mu}^-) \\ &+ i g_{Z_R} (T_R^3 - Y \sin^2 \theta_R) Z_{R\mu}, \end{aligned} \quad (\text{A20})$$

where $T_R^\pm = T_R^1 \pm i T_R^2$. The W_R interaction is the one in the standard model with the left-handed fermions replaced by the right-handed ones. We find the Z_R interaction as

$$\mathcal{L}_{Z_R \bar{f} f} = -g_{Z_R} Z_{R\mu} (c_R^f \bar{f}_R \gamma^\mu f_R + c_L^f \bar{f}_L \gamma^\mu f_L), \quad (\text{A21})$$

where

$$c_R^f = T_R^3 - Y \sin^2 \theta_R, \quad c_L^f = -Y \sin^2 \theta_R, \quad (\text{A22})$$

where $Y(\nu_R) = 0$, $Y(\ell_R) = -1$, $Y(L_L) = -1/2$, $Y(u_R) = 2/3$, $Y(d_R) = -1/3$ and $Y(Q_L) = 1/6$.

5. Gauge coupling constants

The nonstandard gauge coupling constants g_R and $g_{\text{B-L}}$ are related to g_Y by

$$\frac{1}{g_R^2} + \frac{1}{g_{\text{B-L}}^2} = \frac{1}{g_Y^2} = \frac{\cos^2 \theta_W}{4\pi\alpha}. \quad (\text{A23})$$

Thus, we cannot choose g_R and $\sin \theta_R$ independently. Assuming the manifest left-right symmetry $g_R = g_L (= e/\sin \theta_W)$, and taking $\alpha = 1/128$ and $\sin^2 \theta_W = 0.23$, we obtain $g_R = 0.653$ and $\sin^2 \theta_R = 0.299$.

Appendix B: Right-handed neutrino annihilation processes

Processes are listed in the text. We shall give amplitudes and squared amplitudes when relevant helicity states are added.

1. Amplitudes

a. t -channel W_R exchange (a)

$$\mathcal{M}_{t1} = \frac{g_R^2}{2} \frac{1}{t - M_W^2} \mathcal{A}^{(1)}, \quad (\text{B1})$$

$$\mathcal{A}^{(1)} = \bar{u}(q_1) \gamma^\alpha P_R u(p_1) \bar{v}(p_2) \gamma_\alpha P_R v(q_2), \quad (\text{B2})$$

where $t = (p_1 - q_1)^2 = (q_2 - p_2)^2$.

b. t -channel W_R exchange (a)'

$$\mathcal{M}_{t2} = \frac{g_R^2}{2} \frac{1}{t - M_W^2} \mathcal{A}^{(2)}, \quad (\text{B3})$$

$$\mathcal{A}^{(2)} = \bar{u}(q_1) \gamma^\alpha P_R u(p_1) \bar{u}(q_2) \gamma_\alpha P_R u(p_2). \quad (\text{B4})$$

c. s -channel Z_R exchange (b), (b)'

$$\mathcal{M}_{s,fH} = g_{Z_R}^2 c_R^\nu c_H^f \frac{1}{s - M_Z^2} \mathcal{A}_H^{(3)}, \quad (\text{B5})$$

$$\mathcal{A}_H^{(3)} = \bar{v}(p_2) \gamma^\alpha P_R u(p_1) \bar{u}(q_1) \gamma_\alpha P_H v(q_2), \quad (\text{B6})$$

where $s = (p_1 + p_2)^2 = (q_1 + q_2)^2$, $P_{R/L} = (1 \pm \gamma_5)/2$ and $H = R, L$.

d. s -channel W_R exchange (c)

$$\mathcal{M}_s = \frac{g_R^2}{2} \frac{1}{s - M_W^2} \mathcal{A}_R^{(3)}. \quad (\text{B7})$$

2. Squared amplitudes

We evaluate $\overline{\sum} |\mathcal{M}|^2$, where $\overline{\sum}$ means the average of initial spins and sum over final spins in spinor manipulation. It is straight forward to obtain the following squared fundamental amplitudes:

$$\overline{\sum} |\mathcal{A}^{(1)}|^2 = (s + t)^2, \quad (\text{B8})$$

$$\overline{\sum} |\mathcal{A}^{(2)}|^2 = s^2, \quad (\text{B9})$$

$$\overline{\sum} |\mathcal{A}_R^{(3)}|^2 = (s + t)^2, \quad (\text{B10})$$

$$\overline{\sum} |\mathcal{A}_L^{(3)}|^2 = t^2. \quad (\text{B11})$$

We also need the following interference term:

$$\overline{\sum} \mathcal{A}_R^{(3)} \mathcal{A}^{(1)*} = \overline{\sum} \mathcal{A}_R^{(3)*} \mathcal{A}^{(1)} = -(s + t)^2. \quad (\text{B12})$$

These results of helicity-summed squared amplitudes are checked by the software FeynCalc[19] as well.

3. Cross sections

The differential cross section is expressed by

$$d\sigma = \frac{1}{2s\beta_i} \overline{\sum} |\mathcal{M}|^2 d\Phi_2, \quad (\text{B13})$$

where the two-body phase space is given by

$$d\Phi_2 = (2\pi)^4 \delta^4(p_1 + p_2 - q_1 - q_2) \frac{d^3 q_1}{2q_1^0 (2\pi)^3} \frac{d^3 q_2}{2q_2^0 (2\pi)^3}, \quad (\text{B14})$$

$$\int d\Phi_2 = \frac{dt}{8\pi s \beta_i}. \quad (\text{B15})$$

We have performed trivial parts of integration leaving the integration over t variable. In the case of massless particles, $\beta_i = 1$ and the range of integration is $-s \leq t \leq 0$.

a. Right-handed neutrino pair annihilation process (al), (b)

$$\begin{aligned} \sigma^{(1)} = & \frac{1}{16\pi s} \left[\frac{1}{3} g_{Z_R}^4 c_R^{\nu 2} c_R^{\ell 2} \left(\frac{s}{s - M_Z^2} \right)^2 \right. \\ & + \frac{g_R^4}{4} \left\{ 2 + \frac{s}{M_W^2} - 2 \left(1 + \frac{M_W^2}{s} \right) \log \left(1 + \frac{s}{M_W^2} \right) \right\} \\ & - g_R^2 g_{Z_R}^2 c_R^\nu c_R^\ell \frac{s}{s - M_Z^2} \left\{ \frac{3}{2} + \frac{M_W^2}{s} \right. \\ & \left. \left. - \left(1 + \frac{M_W^2}{s} \right)^2 \log \left(1 + \frac{s}{M_W^2} \right) \right\} \right]. \quad (\text{B16}) \end{aligned}$$

In the four-Fermi approximation $M_W \gg s$, using $M_W = M_Z \cos \theta_R$ and $g_R = g_{Z_R} \cos \theta_R$ (namely $\rho_R = 1$), we find

$$\sigma_{4F}^{(1)} = \frac{2}{3\pi} G_R^2 s \left(c_R^\nu c_R^\ell + \frac{1}{2} \right)^2, \quad \frac{G_R}{\sqrt{2}} = \frac{g_R^2}{8M_W^2}. \quad (\text{B17})$$

b. Right-handed neutrino pair annihilation process (b), (b)'

$$\begin{aligned} \sigma^{(2)} = & \frac{n_c}{48\pi s} g_{Z_R}^4 c_R^{\nu 2} c_H^{f 2} \left(\frac{s}{s - M_Z^2} \right)^2, \\ & H = L, R, \quad (\text{B18}) \end{aligned}$$

$$\sigma_{4F}^{(2)} = \frac{2n_c}{3\pi} G_R^2 s c_R^{\nu 2} c_H^{f 2}, \quad (\text{B19})$$

where $n_c (= 3)$ represents the number of colors.

c. *Single right-handed neutrino annihilation process (c)*

$$\sigma^{(3)} = \frac{n_c}{48\pi s} \frac{g_R^4}{4} \left(\frac{s}{s - M_W^2} \right)^2, \quad (\text{B20})$$

$$\sigma_{4\text{F}}^{(3)} = \frac{n_c}{6\pi} G_R^2 s. \quad (\text{B21})$$

d. *Single right-handed neutrino annihilation process (al), (aq)*

$$\sigma^{(4)} = \frac{1}{16\pi s} \frac{g_R^4}{4} \left[2 + \frac{s}{M_W^2} - 2 \left(1 + \frac{M_W^2}{s} \right) \log \left(1 + \frac{s}{M_W^2} \right) \right], \quad (\text{B22})$$

$$\sigma_{4\text{F}}^{(4)} = \frac{1}{6\pi} G_R^2 s. \quad (\text{B23})$$

e. *Single right-handed neutrino annihilation process (a)'*

$$\sigma^{(5)} = \frac{1}{16\pi s} \frac{g_R^4}{4} \frac{s^2}{M_W^4 + sM_W^2}, \quad (\text{B24})$$

$$\sigma_{4\text{F}}^{(5)} = \frac{1}{2\pi} G_R^2 s. \quad (\text{B25})$$

f. *Total cross section*

To summarize, the total ν_R^ℓ annihilation cross section is given by

$$\begin{aligned} \sigma_{4\text{F}} &= \frac{G_R^2 s}{6\pi} \left[5n_c n_g + n_g + 4c_R^\nu \left\{ -c_R^\ell + n_g c_R^\nu \right. \right. \\ &\quad \left. \left. (c_L^{\ell 2} + c_L^{\nu 2} + c_R^{\ell 2} + n_c (c_L^{d 2} + c_L^{u 2} + c_R^{d 2} + c_R^{u 2})) \right\} \right], \\ &= \frac{2G_R^2 s}{\pi} I(\sin^2 \theta_R), \end{aligned} \quad (\text{B26})$$

where $I(x) := (217 - 56x + 40x^2)/48$, and $n_g (= 3)$ represents the number of generations.

Appendix C: Thermal average

We consider the thermal average of cross section σ times (Møller) velocity v :

$$\langle \sigma v \rangle = \frac{g_1 g_2}{n_1 n_2} \int \sigma v f(\mathbf{p}_1) f(\mathbf{p}_2) \frac{d^3 p_1}{(2\pi)^3} \frac{d^3 p_2}{(2\pi)^3}, \quad (\text{C1})$$

$$v := \frac{\sqrt{(p_1 \cdot p_2)^2 - m_1^2 m_2^2}}{E_1 E_2}, \quad (\text{C2})$$

where $g_{1,2}$, $n_{1,2}$ and $f(\mathbf{p}_{1,2})$ denote the spin degrees of freedom, the number densities and the thermal distributions of the initial particles respectively. For the case of massless initial particles, we find $v = s/(2E_1 E_2)$ and

$$\begin{aligned} n &= g \int f(\mathbf{p}) \frac{d^3 p}{(2\pi)^3} \\ &= \frac{3}{4} \zeta(3) \frac{g}{\pi^2} T^3 \simeq 0.90 \frac{g}{\pi^2} T^3, \text{ Fermi-Dirac, } (\text{C3}) \\ &= \frac{g}{\pi^2} T^3, \text{ Maxwell-Boltzmann. } (\text{C4}) \end{aligned}$$

Relation of Fermi-Dirac (FD) and approximate Maxwell-Boltzmann (MB) distribution functions is $f^{\text{FD}} = 1/(e^{E/T} + 1) \rightarrow f^{\text{MB}} = e^{-E/T}$.

1. Maxwell-Boltzmann approximation for initial phase space integration

When the cross section is suppressed for smaller s as in the case of the four-Fermi interaction, we expect that the Maxwell-Boltzmann distribution is a good approximation to the Fermi-Dirac distribution in the thermal average.

To evaluate the thermal integration, the following change of variables is convenient[20]:

$$d^3 p_1 d^3 p_2 = 2\pi^2 E_1 E_2 dE_+ dE_- ds, \quad (\text{C5})$$

where $E_\pm = E_1 \pm E_2$ and the integration region is

$$s > 0, \quad E_+ > \sqrt{s}, \quad |E_-| < \sqrt{E_+^2 - s}, \quad (\text{C6})$$

for the massless case. With the Maxwell-Boltzmann distribution $f(\mathbf{p}) = e^{-E/T}$, we obtain (for the massless case)

$$\langle \sigma v \rangle_{\text{MB}} = \frac{g_1 g_2}{n_1 n_2} \frac{T^2}{32\pi^4} \int \sigma s \frac{\sqrt{s}}{T} K_1(\sqrt{s}/T) ds, \quad (\text{C7})$$

where $K_n(z)$ represents the modified Bessel function of the second kind.

a. *Four-Fermi approximation*

As explicitly shown in the previous section, the cross section is proportional to s in the four-Fermi approximation. We find that the relevant thermal average is given by

$$\langle s v \rangle_{\text{MB}} = \frac{g_1 g_2}{n_1 n_2} \frac{24}{\pi^4} T^8 = 24 T^2, \quad (\text{C8})$$

and

$$\langle \sigma_{4\text{F}} v \rangle_{\text{MB}} = \frac{48 G_R^2 T^2}{\pi} I(\sin^2 \theta_R). \quad (\text{C9})$$

2. Thermal average with Fermi-Dirac distribution

The relevant thermal average using Fermi-Dirac distribution function is

$$\langle sv \rangle_{\text{FD}} = \frac{g_1 g_2}{n_1 n_2} \frac{T^8}{32\pi^4} I_{\text{FD}} \quad (\text{C10})$$

where

$$I_{\text{FD}} = \int d\frac{s}{T^2} d\frac{E_1}{T} \left(\frac{s}{T^2}\right)^2 \frac{\log\left(1 + e^{-s/4(E_1/T)T^2}\right)}{e^{E_1/T} + 1}, \quad (\text{C11})$$

$$= \int_0^\infty dy y^2 \int_0^\infty dx \frac{\log(1 + e^{-y/4x})}{e^x + 1}. \quad (\text{C12})$$

Exchanging the order of x and y integrals, we obtain analytic result given in the text,

$$I_{\text{FD}} = \frac{49\pi^8}{675} \simeq 688.80. \quad (\text{C13})$$

Then, we find

$$\begin{aligned} \langle \sigma_{4F} v \rangle_{\text{FD}} &= \left(\frac{4}{3\zeta(3)}\right)^2 \frac{I_{\text{FD}}}{768} \langle \sigma_{4F} v \rangle_{\text{MB}} \\ &= \frac{49\pi^8}{291600\zeta(3)^2} \langle \sigma_{4F} v \rangle_{\text{MB}} \simeq 1.1035 \langle \sigma_{4F} v \rangle_{\text{MB}} \end{aligned} \quad (\text{C14})$$

Appendix D: Decoupling temperature

The right-handed neutrino annihilation rate is given by $\Gamma = 4n_{\nu_R^c} \langle \sigma v \rangle$. We note that the factor of $4 = 2^2$ is introduced to compensate the initial spin average factor

in the cross sections given in this appendix. In the four-Fermi and Maxwell-Boltzmann approximation, we obtain

$$\Gamma_{4F,\text{MB}} = \frac{192}{\pi^3} G_R^2 T^5 I(\sin^2 \theta_R). \quad (\text{D1})$$

With the Fermi-Dirac distribution, we find

$$\begin{aligned} \Gamma_{4F,\text{FD}} &= \frac{4}{3\zeta(3)} \frac{I_{\text{FD}}}{768} \Gamma_{4F,\text{MB}} = \frac{49\pi^8}{388800\zeta(3)} \Gamma_{4F,\text{MB}} \\ &\simeq 0.99482 \Gamma_{4F,\text{MB}}. \end{aligned} \quad (\text{D2})$$

It turns out that the the Maxwell-Boltzmann approximation is surprisingly accurate. To summarize,

$$\Gamma_{4F,\text{FD(MB)}} = C_{4F,\text{FD(MB)}} G_R^2 T^5 I(\sin^2 \theta_R), \quad (\text{D3})$$

where

$$C_{4F,\text{FD}} = \frac{49\pi^5}{2025\zeta(3)}, \quad C_{4F,\text{MB}} = \frac{192}{\pi^3}. \quad (\text{D4})$$

The decoupling temperature is defined by

$$\Gamma(T_{\text{dec}}) = H(T_{\text{dec}}), \quad H(T) = \sqrt{\frac{8\pi}{3}} \frac{\pi^2}{30} g_* \frac{T^2}{m_{\text{Pl}}}, \quad (\text{D5})$$

where $H(T)$ is the Hubble constant and the Planck mass is $m_{\text{Pl}} = 1.2211 \times 10^{19}$ GeV. We note that $g_* = g_*^{\text{SM}} = 427/4$ for the standard model and $g_* = g_*^{\text{SM}} + 2 \times 3 \times (7/8)$ in the present case.

In the four-Fermi approximation, the right-handed neutrino decoupling temperature is expressed by

$$T_{\text{dec}}^{\nu_R} = \left[\sqrt{\frac{8\pi^3}{90}} g_* \frac{1}{C_{4F,\text{FD(MD)}} G_R^2 m_{\text{Pl}} I(\sin^2 \theta_R)} \right]^{1/3}. \quad (\text{D6})$$

[1] P. Minkowski, Phys.Lett. **B67**, 421 (1977).

The seesaw mechanism is presented in the $SU(2)_R \times SU(2)_L \times U(1)$ framework. This important work has been overlooked in the literature, and the idea was resurrected by many others somewhat later.

[2] M. Fukugita and T. Yanagida, Phys.Lett. **B174**, 45 (1986). This scenario utilizes sphaleron mediated process occurring in thermal medium at several to 10 TeV energy, which partially converts the generated lepton number to the baryon number.

[3] The small contribution 0.046 due to neutrino spectrum distortion at non-instantaneous decoupling is found in G. Mangano, G. Miele, S. Pastor, T. Pinto, O. Pisanti, and P.S. Serpico, Nucl.Phys. **B729**, 221 (2005), arXiv:hep-ph/0506164 [hep-ph] and references therein, is ignored in the present work.

[4] Planck collaboration, N. Aghanim et al., Planck 2018 results. VI. Cosmological parameters, arXiv: 1807.06209. Astron. Astrophys. **641**, A6 (2020)

[5] K. N. Abazajian and J. Heeck, Phys. Rev. **D100**, 075027

(2019).

[6] P. Adshead, Y. Cui, A.J. Long and M. Shamma, Phys. Lett. **B823**, 136736 (2021).

[7] D. Borah, A. Dasgupta, C. Majumdar, D. Nanda, Phys.Rev. **D102**, 035025 (2020).

[8] K.S. Babu, X-G. He, M. Su, and A. Thapa, JHEP **08**, 140 (2022).

[9] CMB-S4 Science Book, arXiv: 1610.02743v1[astro-ph.CO], (2016). Chapter 4 reviews the role of extra ΔN_{eff} that receives contributions from light relics. In particular, Figure 29 of Section 4.4 summarizes BBN result, Planck 2015 result, and CMB-S4 expectations in the (Y_p, N_{eff}) plane.

[10] A.D. Dolgov, Physics Report, **370** 333-535 (2002). See Section 6.4 in particular and references therein. Big-bang nucleosynthesis (BBN) is briefly summarized in Section 3.4.

[11] V. Bernard, S. Descotes-Genon, and L. Vale Silva, JHEP **09**, 088 (2020). arXiv: 2001.00886[hep-ph]

[12] S. Dimopoulos and H. Georgi, Nuclear Physics B. 193,

- 150 (1981).
S. Dimopoulos, S. Raby, and F. Wilczek, *Physical Review D*, **24**, 1681 (1981).
- [13] For an overview of MSSM, see *Perspectives on Supersymmetry II*, Edited By: Gordon L Kane, World Scientific Publishing, Singapore (2010).
- [14] C.S. Aulakh, B. Bajc, A. Melfo, G. Senjanovic, and F. Vissani, *Phys.Lett.B* **588**, 196 (2004).
B. Bajc, A. Melfo, G. Senjanovic, and F. Vissani, *Phys.Lett.B* **634**, 272 (2006).
- [15] I. Esteban, M.C. Gonzalez-Garcia, M. Maltoni, T. Schwetz, and A. Zhou, *The fate of hints: updated global analysis of three-flavor neutrino oscillations*, *JHEP* **09**, 178 (2020); arXiv: 2007.14792 [hep-ph]
- [16] K.S. Babu and R.N. Mohapatra, *Phys. Rev. Lett.* **70**, 2845 (1993), and references therein. This model incorporates the seesaw mass generation due to heavy Majorana neutrinos. We assume that a modification of Higgs potential can lead to the Dirac-type neutrino.
- [17] R. Allison, P. Caucal, E. Calabrese, J. Dunkley, and T. Louis, *Phys. Rev.* **D92**, 123535 (2015). *Towards a cosmological neutrino mass detection*, arXiv: 1509.07471 (2015).
- [18] A. Fukumi, et al, *PTEP* **2012**, 04D002 (2012): e-Print: 1211.4904 [hep-ph].
M. Yoshimura, N. Sasao, and M. Tanaka, *Phys.Rev.***D91**, 063516 (2015): *Experimental method of detecting relic neutrino by atomic de-excitation* arXiv: 1409.3648[hep-ph].
H. Hara, A. Yoshimi, and M. Yoshimura, *Phys.Rev.* **D104**, 115006 (2021). arXiv: 2105.11114 [hep-ph] and references therein.
- [19] V. Shtabovenko, R. Mertig and F. Orellana, *Comput. Phys. Commun.*, **207**, 432-444, 2016, arXiv:1601.01167. "FeynCalc 9.3: New features and improvements", arXiv:2001.04407.
- [20] P. Gondolo and G. Gelmini, *Nucl. Phys.* **B360**, 145 (1991).